

## Activation of monolithic catalysts based on diatomaceous earth for sulfur dioxide oxidation

Esperanza Alvarez<sup>1</sup>, Jesús Blanco<sup>\*</sup>, Pedro Avila, Carlos Knapp

*Instituto de Catálisis y Petroleoquímica, CSIC, Camino de Valdelatas s/n, Cantoblanco, 28049 Madrid, Spain*

### Abstract

The formation of the active phases during the activation process of monolithic catalysts based on  $V_2O_5$ – $K_2SO_4$  supported on diatomaceous earth for  $SO_2$  to  $SO_3$  oxidation in flue gases, has been shown to be a crucial factor to achieve satisfactory catalytic performance. As the temperature is increased from room temperature to  $470^\circ\text{C}$ ,  $SO_2$  and  $SO_3$  are taken up by the green catalyst and the precursors are transformed into the active species. The role of each component of the catalyst during the activation was analyzed by studying the behavior towards  $SO_2$  adsorption of four materials, which contained: diatomaceous earth, diatomaceous earth + V, diatomaceous earth + K, and diatomaceous earth + V + K. The influence of the potassium sulfate accessibility in the green catalyst was studied by using two different preparation methods, which gave rise to differences in the catalysts  $SO_2$  adsorption properties and catalytic performance. Furthermore, the influence of the activation atmosphere was studied using nitrogen, oxygen or a flue gas composition. It was shown that pyrosulfate species should be formed at temperatures below  $400^\circ\text{C}$ , to keep the vanadium in the active 5+ oxidation state. ©1999 Elsevier Science B.V. All rights reserved.

*Keywords:* Monolith; Sulfur dioxide oxidation;  $DeSO_x$ ; Catalyst activation

### 1. Introduction

The  $SO_2$  contribution to the acid rain phenomena and its pernicious effects on ecosystems and human health have reinforced the development of more efficient cleaning technologies for the treatment of industrial gaseous emissions.

The catalytic oxidation of  $SO_2$  traces to  $SO_3$  seems to be one of the most feasible ways to carry out the desulfurization of flue gas from power stations. The catalyst commonly used in this  $SO_2$  oxidation pro-

cess corresponds to supported vanadium–alkali complex sulfates compounds which has been described as a molten–salt/gas  $M_2S_2O_7/V_2O_5/SO_2/SO_3$  system, where  $M = \text{Na, K and/or Cs}$ .

Different research teams have been working in the characterization of the active species of these supported liquid phase (SLP) catalysts using various techniques, such as IR spectroscopy [1], ESR [2,3], Raman spectroscopy [4], potentiometry, cryoscopy, and spectrophotometry [5], calorimetry [6], density measurement and conductimetry [7] and NMR spectroscopy [8,9]. Although Fehrmann and co-workers have studied the phase changes in the temperature range  $20$ – $550^\circ\text{C}$  for  $Cs_2S_2O_7$ – $V_2O_5$  [10] and  $K_2S_2O_7$ – $V_2O_5$  [11] systems, little is known about the activation of the active phase precursors, which would be expected to have influence on the performance of the final catalyst.

<sup>\*</sup> Corresponding author. Tel.: +34-91-585-48-02; fax: +34-91-585-47-89

E-mail address: jblanco@icp.csic.es (J. Blanco)

<sup>1</sup> Present address: SRI International, 333 Ravenswood Avenue, Menlo Park, CA 94025, USA.

In a previous work, the performance of this catalyst supported on a diatomaceous earth with monolithic geometry was tested for the treatment of flue gases from power stations; the results indicated that, at  $T = 450^\circ\text{C}$ ,  $P = 120\text{ kPa}$ ,  $\text{GHSV (NTP)} = 4900\text{ h}^{-1}$ ,  $[\text{SO}_2] = 1000\text{ ppm}$ , and  $[\text{O}_2] = 5\text{ vol}\%$ ,  $\text{SO}_2$  conversions higher than 80% might be achieved, if the previous activation of the catalyst is carried out properly [12].

The aim of the present work has been to study the different steps of the green catalyst activation process, which take place as the temperature is increased from room temperature to  $470^\circ\text{C}$ , the  $\text{SO}_2$  and  $\text{SO}_3$  are taken up by the green catalyst, and consequently the precursors are transformed into the active species.

## 2. Experimental

### 2.1. Catalysts preparation

A calcined diatomaceous earth (82 wt%  $\text{SiO}_2$ , 7.0 wt%  $\text{Na}_2\text{O}$ , 3.0 wt%  $\text{Al}_2\text{O}_3$ , 2.3 wt%  $\text{Fe}_2\text{O}_3$ , 1.2 wt%  $\text{CaO}$ , 0.7 wt%  $\text{TiO}_2$ , 0.3 wt%  $\text{MgO}$ , 0.3 wt%  $\text{K}_2\text{O}$ , 3.2 wt% other oxides) was used as support; potassium sulfate (99.94 wt%  $\text{K}_2\text{SO}_4$ , <0.7 wt%  $\text{Cl}^-$ , 4 wt%  $\text{H}_2\text{SO}_4$ , <0.2 wt%  $\text{H}_2\text{O}$ ) and ammonium metavanadate (99 wt%  $\text{NH}_4\text{VO}_3$ , <0.2 wt%  $\text{Cl}^-$ , <0.05 wt%  $\text{SO}_4^{2-}$ , <0.3 wt%  $\text{CO}_3^{2-}$ ) were used as potassium and vanadium precursors, respectively.

The catalysts were manufactured by extrusion of doughs prepared by two different procedures. In method A, the dough was prepared by kneading a mixture of diatomaceous earth and potassium sulfate powders, with an ammonium metavanadate aqueous suspension, to which oxalic acid was added to dissolve the salt. In method B, the potassium sulfate powder was added to vanadium salt aqueous solution, subsequently kneading the suspension with the diatomaceous earth powder to obtain the dough. In both procedures the obtained square-cell monoliths, after activation, had a cell density of  $7.7\text{ cells cm}^{-2}$ , pitch of 0.36 cm, wall thickness of 0.09 cm, geometric surface area of  $833\text{ m}^2\text{ m}^{-3}$ , bulk density of  $0.7\text{ g cm}^{-3}$  and a crushing strength of around  $470\text{ kg cm}^{-2}$ . The V/K atomic ratio was 3.5, and the  $\text{V}_2\text{O}_5$  content 7.4 wt%.

Furthermore, monoliths with similar geometry were prepared from some of the materials used for the cat-

Table 1  
Composition by weight of the 6 cm length monolithic samples (g) before treatment

Sample	Diatomaceous earth	$\text{K}_2\text{SO}_4$	$\text{NH}_4\text{VO}_3$	Total
1	1.149	–	–	1.149
2	0.861	0.362	–	1.223
3	0.941	–	0.140	1.081
4	0.937	0.394	0.139	1.470

alysts manufacture. The compositions by weight of these samples are shown in Table 1.

### 2.2. Activation and activity tests

Studies on the  $\text{SO}_2$  adsorption capacity of the monolithic samples shown in Table 1 were carried out using a single channel of 6 cm length placed in a stainless-steel micro-reactor, operating with an inlet composition of:  $[\text{SO}_2] = 700\text{ ppm}$ ,  $[\text{O}_2] = 3\text{ vol}\%$  and  $[\text{Ar}] = \text{balance}$ , at a pressure of 107 kPa and GHSV (gas hourly space velocity, at normal conditions) of  $3660\text{ h}^{-1}$ . The temperature was increased at a rate of ca.  $5^\circ\text{C min}^{-1}$  from room temperature to  $470^\circ\text{C}$ . The detection and quantification of  $\text{SO}_2$  at the micro-reactor inlet and outlet was performed by mass spectrometry (Balzers Omnistar), using a channeltron detector.

The activation of the catalyst with different gas compositions and the catalytic activity measurements were carried out in a monolithic reactor working close to the isothermal axial profile, with gas mixtures containing  $[\text{SO}_2] = 0 - 700\text{ ppm}$ ,  $[\text{O}_2] = 0 - 21\text{ vol}\%$ , and  $[\text{N}_2] = \text{balance}$ , at the following operation conditions: temperature =  $25 - 470^\circ\text{C}$ , pressure = 107 kPa and GHSV =  $3200\text{ h}^{-1}$ ;  $\text{SO}_2$  contents were analyzed by Gas Chromatography (Varian 3400), using a photometric detector, and  $\text{SO}_3$  measurements were carried out by volumetric analysis [13].

### 2.3. Characterization techniques

Laser Raman spectroscopy was used to study the samples surface compositions after use. The spectra were performed on the monolith walls at room temperature, with a Bruker RFS 100 spectrometer, exciting at 1046 nm with a Nd:YAG laser source. A germanium

diode cooled with liquid nitrogen was used for detection, with a resolution of  $4\text{ cm}^{-1}$ . Laser power of 100–500 mW was used during the measurements. Before the measurements, the samples were irradiated for 2 h with a normal tungsten lamp, in order to reduce interference by the sample fluorescence.

The pore volumes were determined by use of mercury intrusion porosimetry (MIP) using CE Instruments Pascal 140/240 porosimeters. For these measurements, the values recommended by the IUPAC [14] of contact angle  $141^\circ$  and surface tension  $484\text{ mNm}^{-1}$  were used.

### 3. Results and discussion

#### 3.1. Short-term $\text{SO}_2/\text{O}_2$ treatment

The  $\text{SO}_2$  adsorption of the four materials shown in Table 1, as the temperature was increased at ca.  $5^\circ\text{C min}^{-1}$  up to  $470^\circ\text{C}$  and subsequently maintained at this latter temperature, is shown in Fig. 1 for the first 2 h in operation.

At low temperature (20– $100^\circ\text{C}$ ) the four samples adsorbed large quantities of  $\text{SO}_2$ , which corresponds to physical  $\text{SO}_2$  adsorption, and the adsorbed amount could be related to the pore volume of the samples, determined by mercury intrusion porosimetry: diatomaceous earth +  $\text{NH}_4\text{VO}_3$  ( $0.35\text{ ml g}^{-1}$ ) > diatomaceous earth ( $0.33\text{ ml g}^{-1}$ ) > diatomaceous earth +  $\text{K}_2\text{SO}_4$  ( $0.31\text{ ml g}^{-1}$ ) > diatomaceous earth +  $\text{K}_2\text{SO}_4$  +  $\text{NH}_4\text{VO}_3$  ( $0.26\text{ ml g}^{-1}$ ).

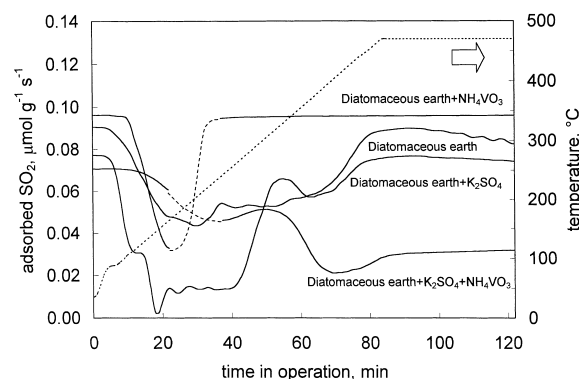


Fig. 1. Adsorbed  $\text{SO}_2$  and operating temperature as a function of time in operation of the monolithic samples.  $[\text{SO}_2] = 700\text{ ppm}$ ,  $[\text{O}_2] = 3\text{ vol}\%$ ,  $[\text{Ar}] = \text{balance}$ ; GHSV =  $3660\text{ h}^{-1}$ ,  $P = 107\text{ kPa}$ .

#### 3.1.1. Diatomaceous earth

After a decrease of  $\text{SO}_2$  uptake above  $100^\circ\text{C}$ , at  $350^\circ\text{C}$  an increase in  $\text{SO}_2$  consumption was observed, which can be assigned to the formation of sulfates from some of the oxides present in this material as impurities.

#### 3.1.2. Diatomaceous earth + $\text{K}_2\text{SO}_4$

When potassium sulfate was added to the diatomaceous earth, a similar temperature/adsorption profile was observed up to  $200^\circ\text{C}$ , although the adsorption was lower than that observed with the diatomaceous. This decrease is probably due to a partial clogging of the diatomaceous earth inter- and intraparticle pores by the potassium sulfate. A further increase of the temperature above  $250^\circ\text{C}$  led to higher adsorption, reaching a maximum at  $330^\circ\text{C}$ . This has been explained by the initiation of the  $\text{K}_2\text{S}_2\text{O}_7$  formation by reaction of the  $\text{K}_2\text{SO}_4$  with  $\text{O}_2$  and  $\text{SO}_2$ , increasing the uptake of the latter; as  $\text{K}_2\text{SO}_4$  and  $\text{K}_2\text{S}_2\text{O}_7$  are solid at temperatures below  $420^\circ\text{C}$ , this phenomenon would be expected to occur only on the  $\text{K}_2\text{SO}_4$  particles surface. The presence of any  $\text{KHSO}_4$  impurities would increase this effect, by decreasing the melting point of the mixture, according to the phase diagram of the  $\text{K}_2\text{S}_2\text{O}_7$ – $\text{KHSO}_4$  [15].

#### 3.1.3. Diatomaceous earth + $\text{NH}_4\text{VO}_3$

After adsorption at low temperature (assigned to physical adsorption), the sample containing diatomaceous earth and the vanadium lost  $\text{NH}_3$  from  $170^\circ$  to  $220^\circ\text{C}$ . Above  $220^\circ\text{C}$ , a fairly constant  $\text{SO}_2$  adsorption was observed, as vanadyl sulfate ( $\text{VOSO}_4$ ) was starting to be formed.

The Raman spectrum of this sample (Fig. 2) shows not only the presence of characteristic  $\text{V}_2\text{O}_5$  bands at 995, 706, 286, 200 and  $145\text{ cm}^{-1}$ , but also the appearance of  $\text{VOSO}_4$  ( $974\text{ cm}^{-1}$ ). A similar behavior has been previously reported by Ivanenko et al. [16], who observed that the sulfation of  $\text{V}_2\text{O}_5$  on silica led to the reduction of V(V) to V(IV) by the transformation of  $\text{V}_2\text{O}_5$  to  $\text{VOSO}_4$ , at temperatures above  $400^\circ\text{C}$ .

#### 3.1.4. Diatomaceous earth + $\text{K}_2\text{SO}_4$ + $\text{NH}_4\text{VO}_3$

The observations described above help to understand some steps of the activation pattern of the green catalyst: the  $\text{SO}_2$  adsorption at low temperature

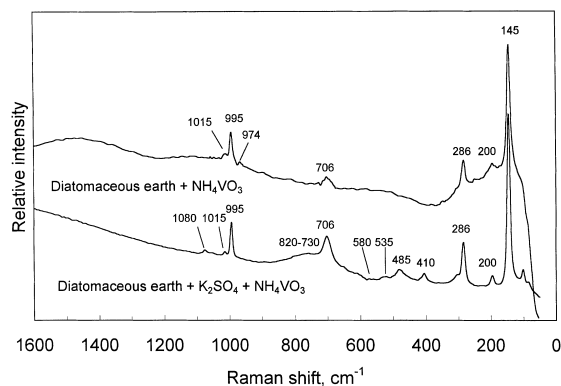


Fig. 2. Raman spectra of the vanadium containing samples after activation in  $[\text{SO}_2] = 700$  ppm,  $[\text{O}_2] = 3$  vol%,  $[\text{Ar}] = \text{balance}$ , for 2 h; GHSV =  $3660 \text{ h}^{-1}$ ;  $P = 107$  kPa;  $T = 25\text{--}470^\circ\text{C}$  (increasing rate ca.  $5^\circ\text{C min}^{-1}$ ).

( $25\text{--}100^\circ\text{C}$ ) due to physical adsorption, the exit of  $\text{NH}_3$  from ammonium vanadate decomposition ( $170\text{--}220^\circ\text{C}$ ), and the formation of potassium pyrosulfate ( $250\text{--}370^\circ\text{C}$ ). However, the presence of the vanadium and potassium precursors simultaneously will give rise to alkali pyrosulfates which regenerate the active species V(V) by oxidation of V(III) and V(IV), that otherwise lead to deactivation of the catalyst [17]. The Raman spectrum of this sample (Fig. 2) shows characteristic  $\text{S}_2\text{O}_7$  bands at 1080 and  $730\text{--}820 \text{ cm}^{-1}$  [18], besides other  $\text{V}_2\text{O}_5$  characteristic bands (995, 706, 286, 200 and  $145 \text{ cm}^{-1}$ ), and a band at  $1015 \text{ cm}^{-1}$  that has been generally assigned to surface vanadyl groups [19]. However, the  $\text{VO}_2$  ( $974 \text{ cm}^{-1}$ ) is not observed. Above  $330^\circ\text{C}$ , the  $\text{K}_2\text{S}_2\text{O}_7\text{--V}_2\text{O}_5$  eutectic would start to be formed [11,20] and fusion would take place, initiating the formation of the catalyst's liquid active phase. The  $\text{SO}_2$  diffusion in the liquid phase would be less effective, and might be the cause for lower  $\text{SO}_2$  adsorption observed in the  $300\text{--}400^\circ\text{C}$  range.

### 3.2. Long-term $\text{SO}_2/\text{O}_2$ treatment

Fig. 3 shows the accumulated  $\text{SO}_2$  amounts as a function of time in operation when feeding with a gas mixture containing 700 ppm  $\text{SO}_2$  and 3 vol%  $\text{O}_2$ , obtained with the four samples. The support (*diatomaceous earth*) tended to achieve a constant value after

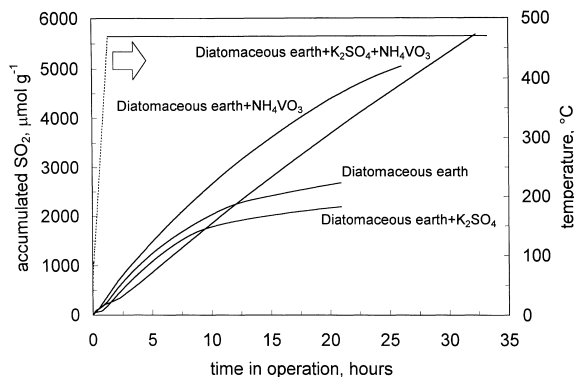


Fig. 3. Accumulated quantity of  $\text{SO}_2$  and operating temperature as a function of time in operation of the monolithic samples.  $[\text{SO}_2] = 700$  ppm,  $[\text{O}_2] = 3$  vol%,  $[\text{Ar}] = \text{balance}$ ; GHSV =  $3660 \text{ h}^{-1}$ ;  $P = 107$  kPa.

20 h, indicating saturation of the sorption sites, ca.  $0.192 \text{ gSO}_2 \text{ g}_{\text{solid}}^{-1}$ .

When adding  $\text{K}_2\text{SO}_4$  (*diatomaceous earth* +  $\text{K}_2\text{SO}_4$ ), also saturation was observed, although the total accumulated quantity was lower (ca.  $0.140 \text{ gSO}_2 \text{ g}_{\text{solid}}^{-1}$ ), indicating a pore clogging effect, as mentioned above.

The *diatomaceous earth* +  $\text{NH}_4\text{VO}_3$  sample accumulated larger quantities of  $\text{SO}_2$ , through the formation of vanadium sulfate. This would lead to a decrease in activity, due to the reduction of the catalyst active species, V(V), to lower undesired oxidation state. Additionally, some slight conversion of  $\text{SO}_2$  to  $\text{SO}_3$  has been observed.

In the case of the catalyst, *diatomaceous earth* +  $\text{K}_2\text{SO}_4$  +  $\text{NH}_4\text{VO}_3$ , a continuous  $\text{SO}_2$  accumulation/disappearance was observed, in which the  $\text{SO}_2$  adsorption rate would be gradually substituted by the  $\text{SO}_2$  to  $\text{SO}_3$  conversion, as will be discussed later.

### 3.3. Influence of the potassium sulfate accessibility

The catalyst was prepared by two different methods, in which the only difference was the way in which potassium sulfate was added. In method A, the  $\text{K}_2\text{SO}_4$  was added to the diatomaceous earth powder, while in method B the addition was made to the vanadium salt aqueous solution. The catalyst prepared by method B adsorbed lower quantities of  $\text{SO}_2$  than that prepared by method A. The  $\text{SO}_2$  conversions values for both

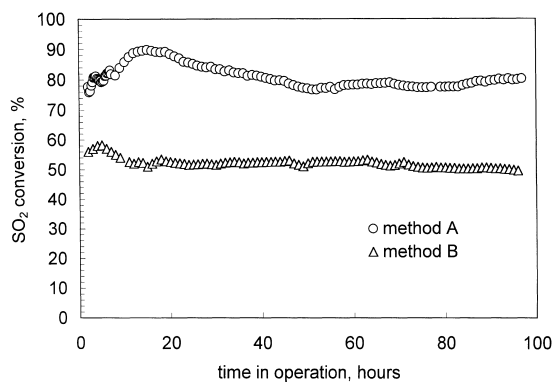


Fig. 4.  $\text{SO}_2$  conversions at  $470^\circ\text{C}$  of monolithic catalysts prepared by two different methods as a function of time in operation;  $[\text{SO}_2]=700$  ppm,  $[\text{O}_2]=3$  vol%,  $[\text{N}_2]=$  balance; GHSV =  $3200\text{ h}^{-1}$ ;  $P=107$  kPa.

catalysts shown in Fig. 4, clearly demonstrate that method A led to a much more active catalyst.

When the potassium sulfate particles are introduced into the vanadium salt solution — method B —, most of them might be covered by a vanadium salt layer that will limit their direct contact with  $\text{SO}_2$  or  $\text{O}_2$  during the activation process. With method A, however, the formation of the active phase is more favorable as the  $\text{SO}_2$  has high accessibility to the potassium sulfate, which would be able to stabilize the V(V) as it is transformed to pyrosulfates at temperatures below  $400^\circ\text{C}$ . This was confirmed by Raman spectroscopy, as the catalyst prepared by method B showed much weaker  $\text{V}_2\text{O}_5$  bands than the one prepared by method A (which showed a spectrum similar to the one presented in Fig. 2 as *Diatomaceous earth* +  $\text{K}_2\text{SO}_4$  +  $\text{NH}_4\text{VO}_3$ ).

The ratio between  $\text{V}_2\text{O}_5$  and  $\text{K}_2\text{SO}_4$  and the operation temperature have been pointed out as the two main parameters to be taken into account when designing catalysts for  $\text{SO}_2$  to  $\text{SO}_3$  oxidation [21]. The present results indicate that another important aspect might be the accessibility of the potassium sulfate, which allows an adequate pyrosulfate formation, leading to the  $\text{V}_2\text{O}_5$  stabilization.

### 3.4. Influence of the activation atmosphere

The influence of the gas composition during the activation process on the catalyst activity was studied using the catalyst prepared by method A. In

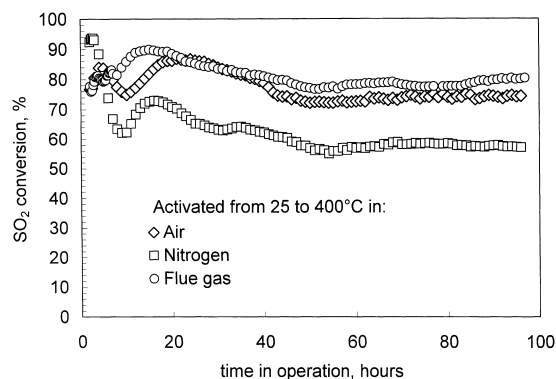


Fig. 5.  $\text{SO}_2$  conversions at  $470^\circ\text{C}$  of the monolithic catalyst (method A) after activation in different atmospheres, as a function of time in operation.  $[\text{SO}_2]=700$  ppm,  $[\text{O}_2]=3$  vol%,  $[\text{N}_2]=$  balance; GHSV =  $3200\text{ h}^{-1}$ ;  $P=107$  kPa.

these experiments, the activation step was carried out in a flow of air, nitrogen, or an  $\text{SO}_2/\text{O}_2$  mixture with a typical composition of a power plant flue gas ( $[\text{SO}_2]=700$  ppm,  $[\text{O}_2]=3$  vol%,  $[\text{N}_2]=$  balance) increasing the temperature from  $25$  to  $400^\circ\text{C}$ , at a rate of ca.  $5^\circ\text{C min}^{-1}$ . When  $400^\circ\text{C}$  were achieved, the flue gas was fed into the reactor, and the temperature was further increased up to  $470^\circ\text{C}$ , in all cases. The  $\text{SO}_2$  conversions are shown in Fig. 5 as a function of time in operation. In the three cases, total stabilization was reached only after ca. 50 h in operation. The highest conversion, 80%, was obtained when the activation step was carried out with the flue gas composition; 75% when air was used, and 57% if the activation process was carried out in nitrogen.

These results show that the key transformations that take place in the catalyst during the activation step are strongly affected by the presence of oxygen and  $\text{SO}_2$ . Activating in nitrogen would allow reduction of V(V) into undesired V(IV) and V(III) due to the presence of reducing agents, such as oxalic acid. If the activation is carried out in an oxidizing atmosphere (21 vol%  $\text{O}_2$ ), the V(V) is stabilized; but when  $\text{SO}_2$  is added at temperatures above  $400^\circ\text{C}$ , some may react with the  $\text{V}_2\text{O}_5$  to form vanadyl sulfate with loss of catalytic activity. Therefore, the presence of  $\text{SO}_2/\text{O}_2$  at temperatures below  $400^\circ\text{C}$  allowing the formation of the pyrosulfate species ( $320$ – $370^\circ\text{C}$ ), which will give rise to the formation of the eutectic active composition [22], maintaining the stability of the V(V) state, is important.

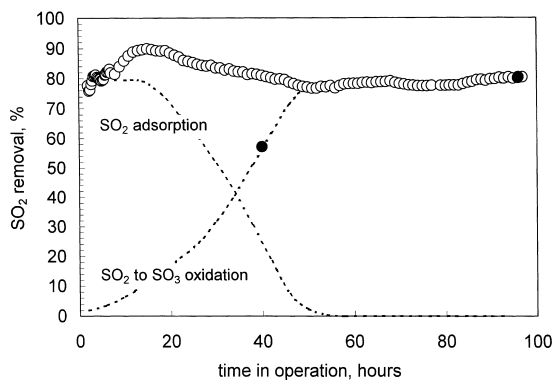


Fig. 6. Simultaneous  $\text{SO}_2$  adsorption and  $\text{SO}_2$  oxidation during the monolithic catalyst activation: (○) experimental  $\text{SO}_2$  conversion, (●) experimental  $\text{SO}_3$  formation, and (---) estimated  $\text{SO}_2$  adsorption and  $\text{SO}_2$  oxidation values.  $[\text{SO}_2]=700$  ppm,  $[\text{O}_2]=3$  vol%,  $[\text{N}_2]=$  balance.  $T=470^\circ\text{C}$ ;  $\text{GHSV}=3200\text{ h}^{-1}$ ;  $P=107$  kPa.

### 3.5. $\text{SO}_2$ adsorption vs. $\text{SO}_2$ oxidation

The long-term  $\text{SO}_2$  disappearance can be interpreted in terms of an addition of both an  $\text{SO}_2$  adsorption that gives rise to the formation of the active phases, and the initiation of the  $\text{SO}_2$  to  $\text{SO}_3$  oxidation by these newly generated species. In Fig. 6, the two processes are distinguished for catalyst A activated with a gas containing 700 ppm  $\text{SO}_2$  and 3 vol%  $\text{O}_2$ . During the first 60 h, the monolith adsorbs  $\text{SO}_2$  at a rate which decreases with the time in operation as the active phase is being formed. Meanwhile, the active phases start to transform  $\text{SO}_2$  to  $\text{SO}_3$  at an increasing rate, as was confirmed by determination of the  $\text{SO}_3$  concentration at the reactor outlet, achieving the stable value that is observed on right side of the figure.

## 4. Conclusions

The results obtained in the activation studies with monolithic catalysts for  $\text{SO}_2$  to  $\text{SO}_3$  oxidation based on  $\text{V}_2\text{O}_5\text{-K}_2\text{SO}_4$  supported on diatomaceous earth, indicate that the formation of the active phases is a crucial process in order to achieve satisfactory catalytic activities.

During this *activation process* it is necessary to form pyrosulfate species, which keep the vanadium in the

active 5+ oxidation state, for which the following aspects should be taken into account:

- the activation should be carried out in oxidizing atmosphere and in the presence of  $\text{SO}_2$ .
- the formation of the pyrosulfate should take place as soon as possible, in order to limit the formation of vanadyl sulfate —  $\text{V(IV)}$  —, which will diminish the catalyst activity.
- the  $\text{K}_2\text{SO}_4$  should be as accessible as possible to the  $\text{SO}_2$  and  $\text{O}_2$ , at temperatures between  $300^\circ$  and  $400^\circ\text{C}$ .
- the presence of reducing agents such as CO or hydrocarbons during the activation process, would have a negative influence, as they will reduce the oxidation state of  $\text{V(V)}$ .

## Acknowledgements

This work was supported by the CAM (Comunidad Autónoma de Madrid), Project 0057/94 and by CECA-EU, Project 7220-ED/080. We wish to thank the members of SRI International's Material Research Laboratory (USA) for valuable support. Dr. E. Alvarez thanks the Ministry of Education and Science of Spain for a research fellow grant. We are also grateful to Dr. R. Valenzuela and Dr. V. Cortés for their help in obtaining the Raman spectra, and to Dr. M. Yates for valuable discussions.

## References

- [1] S. Boghosian, R. Fehrmann, N.J. Bjerrum, G.N. Papatheodorou, *J. Catal.* 119 (1989) 121–134.
- [2] L.G. Simonova, Y.O. Bulgakova, O.B. Lapina, B.S. Bal'zhinimaev, *Kinetics and Catalysis* 38 (1997) 820–824.
- [3] S.G. Masters, K.M. Eriksen, R. Fehrmann, *J. Mol. Catal. A* 120 (1997) 227–233.
- [4] S. Boghosian, F. Borup, A. Chrissanthopoulos, *Catal. Lett.* 48 (1997) 145–150.
- [5] N.H. Hansen, R. Fehrmann, N.J. Bjerrum, *Inorg. Chem.* 21 (1982) 744–752.
- [6] R. Fehrmann, M. Gaune-Escard, N.J. Bjerrum, *Inorg. Chem.* 25 (1986) 1132.
- [7] G. Hatem, R. Fehrmann, M. Gaune-Escard, N.J. Bjerrum, *J. Phys. Chem.* 91 (1987) 195–203.
- [8] V.M. Mastikhin, O.B. Lapina, L.G. Simonova, *React. Kinet. Catal. Lett.* 26 (1984) 431–436.
- [9] D.A. Karydis, K.M. Eriksen, R. Fehrmann, S. Boghosian, *J. Chem. Soc. Dalton. Trans* (1994) 2151–2157.

- [10] O.B. Lapina, V.V. Terskikh, A.A. Shubin, V.M. Mastikhin, K.M. Eriksen, R. Fehrmann, *J. Phys. Chem. B* 101 (1997) 9188–9194.
- [11] G.E. Folkmann, K.M. Eriksen, R. Fehrmann, M. Gaune-Escard, G. Hatem, O.B. Lapina, V. Terskikh, *J. Phys. Chem. B* 102 (1998) 24–28.
- [12] J. Blanco, A. Bahamonde, E. Alvarez, P. Avila, *Catal. Today* 42 (1998) 85–92.
- [13] *Methods of Air Sampling and Analysis*, 2nd ed., Am. Pub. Health Assn., Washington, DC, 1977, p. 737.
- [14] J. Rouquerol, D. Avnir, C.W. Firbridge, D.H. Everett, J.H. Haynes, N. Pernicone, J.D.F. Ramsay, K.S.W. Sing, K.K. Unger, *Pure and Appl. Chem.*, 66 (1994) 1739.
- [15] K.M. Eriksen, R. Fehrmann, G. Hatem, M. Gaune-Escard, O.B. Lapina, V.M. Mastikhin, *J. Phys. Chem.* 100 (1996) 10771–10778.
- [16] S.V. Ivanenko, R.R. Dzhoraev, *Kinetics and Catalysis* 35 (1994) 581–583.
- [17] G.H. Tandy, *J. Appl. Chem.* 6 (1956) 68–74.
- [18] R. Fehrmann, N.H. Hausen, N.J. Bjerrum, *Inorg. Chem.* 22 (1983) 4009–4014.
- [19] B. Handy, A. Baiker, M. Scharml-Marth, A. Wokaun, *J. Catal.* 133 (1992) 1–20.
- [20] S. Hähle, A. Meisel, *Kinetics and Catalysis* 12 (1971) 1132–1136.
- [21] J. Villadsen, H. Livbjerg, *Catal. Rev.-Sci. Eng.* 17 (1978) 203–272.
- [22] V.M. Mastikhin, O.B. Lapina, B.S. Balzhinimaev, L.G. Simonova, L.M. Karnatovskaya, A.A. Ivanova, *J. Catal.* 103 (1987) 160–169.